NEOPLASIA
www.neoplasia.com

Volume 10 Number 8 August 2008 pp. 838–846 838

Molecular Credentialing of Rodent Bladder Carcinogenesis Models[1]

Paul D. Williams*, Jae K. Lee* and Dan Theodorescu†

*Department of Public Health Sciences, Division of Biostatistics, University of Virginia School of Medicine, Charlottesville, VA 22908-0717, USA; †Department of Molecular Physiology and Biological Physics, University of Virginia School of Medicine, Charlottesville, VA 22908, USA

Abstract

Cancer of the urinary bladder is often a result of exposure to chemical carcinogens. Models of this disease have been developed by exposing rodents to *N*-butyl-*N*-(4-hydroxybutyl)-nitrosamine (OH-BBN). The resultant tumors are histologically similar to human disease, but little is known about genetic similarities to the latter. Such knowledge would help identify or corroborate genes found important in human bladder cancer and suggest biologically appropriate mechanistic studies. We address this need by comparing gene expression profiles associated with urothelial carcinoma for three different species: mouse, rat, and human. We find that many human genes homologous to those differentially expressed in carcinogen-induced rodent tumors are also differentially expressed in human disease and are preferentially associated with progression from non–muscle-invasive to muscle-invasive disease. We also find that overall gene expression profiles of rodent tumors correspond more closely with those of invasive human tumors rather than non–muscle-invasive tumors. Finally, we provide a list of genes that are likely candidates for driving this disease process by virtue of their concordant regulation in tumors of all three species.

Neoplasia (2008) 10, 838–846

Introduction

Cancer of the urinary bladder is the fourth most common newly diagnosed cancer in men in the United States, with 51,230 new diagnoses predicted in 2008, and will be responsible for an estimated 14,100 deaths [1]. Most bladder tumors in the western world are of urothelial ("transitional") cell histology and are categorized according to cellular grade and the extent to which the tumor invades the surrounding tissues. The prognosis is good for those with non–muscle-invasive tumors, whereas those with muscle-invasive disease are at increased risk of metastasis and death [2]. Having robust and clinically relevant animal models for the mechanistic study of the causes underlying carcinogenesis, tumor progression, and metastasis of urothelial carcinoma would improve treatment and prognosis for patients with bladder cancer.

Many bladder cancers result from exposure to chemical carcinogens. It is estimated that one third to one half of bladder tumors are associated with cigarette smoking [3,4]. Whereas the specific causative agent in cigarette smoke remains unidentified, α- and β-naphthylamine are suspected. Occupational exposure to aromatic amines such as β-naphthylamine, 4-aminobiphenyl, benzidine, and 2-amino-1-naphthol, among other chemicals, accounts for an additional 20% to 30% of bladder cancer cases in the United States [5,6].

Given the importance of chemical carcinogenesis to the development of bladder cancer, we sought to evaluate the degree of molecular similarity of two commonly used primary rodent models of this disease to human bladder cancer. Both models involve the administration of *N*-butyl-*N*-(4-hydroxybutyl)-nitrosamine (OH-BBN) to mice [7,8] or rats [9–11]. Second, if molecular similarity did exist, we sought to determine, by virtue of cross-species comparison, which genes were the most important in bladder tumor development and progression, thus providing promising leads for future research. Experiments profiling the gene expression of normal urothelium and OH-BBN–induced

Address all correspondence to: Dan Theodorescu, Department of Molecular Physiology and Biological Physics, Box 800422, University of Virginia School of Medicine, Charlottesville, VA 22908. E-mail: theodorescu@virginia.edu

[1]This work was supported by National Institutes of Health grants T32DK069264 to P.D.W. and R01CA075115 to D.T.
Received 1 April 2008; Revised 5 May 2008; Accepted 8 May 2008

DOI 10.1593/neo.08432

bladder tumors in both rat and mice have been published [12,13], providing an opportunity to address these important questions.

Methods

Human Bladder Cancer Microarrays

We constructed a human bladder cancer gene expression data set of 53 previously published Affymetrix HG-U133A GeneChips, including normal urothelial tissue and both non–muscle-invasive and muscle-invasive tumors. Data from 30 microarray chips were downloaded from the Gene Expression Omnibus Web site (GEO Accession Number GSE3167) [14–16], whereas those of 23 chips were obtained locally [17]. The clinical characteristics of the characterized tissues are summarized in Table 1. Microarray profiles were classified according to the type of tissue hybridized to the chip. Fifteen chips were hybridized with RNA from normal urothelium, 14 chips with non–muscle-invasive bladder tumors (defined as stage Ta or T1 tumors with grade less than 3), and 24 chips with muscle-invasive bladder tumors (defined as stage T2 or greater, any grade). We used the Robust Multichip Average method to quantile-normalize, background-adjust, and summarize the gene expression values from these chips [18–20].

Rodent Bladder Cancer Microarrays

Yao et al. [12] found 1554 mouse genes differentially expressed between bladder cancer and normal urothelial tissue with a *t* test *P* value < .05 and fold change ≥ 2, 867 of which were overexpressed and 687 underexpressed in the tumors. They published 53 overexpressed and 37 underexpressed genes along with fold change values. In a similar study, they found 1138 rat genes to be differentially expressed with a *t* test *P* value < .05 and fold change ≥ 2, 770 of which were overexpressed and 368 underexpressed in the tumors. They published 98 overexpressed and 47 underexpressed genes or transcripts with fold change values [13].

Homology and Statistical Analysis of Bladder Cancer Microarrays

We used the NetAffx information site (http://www.affymetrix.com) to determine which human Affymetrix HG-U133A probe sets were homologous with the published rodent genes [21] (Figure 1*A*). Because Yao et al. [12] used Affymetrix MG-U74Av2 and Rat 230 2.0 GeneChips to measure gene expression in the normal and cancerous tissues, we first determined which MG-U74Av2 probe sets correspond to the accession numbers of the listed mouse genes and which Rat 230 2.0 probe sets correspond to the listed rat genes or transcript accession numbers. We then found the HG-U133A probe sets that were homologous to these matched mouse and rat genes. Some rodent genes had multiple human homologs, whereas others had none. No human probe sets were homologous to more than one mouse or rat gene, with the exception of 201429_s_at and 202240_at, which were homologous to *Plk* and *Plk-ps1*. Because *Plk-ps1* is a pseudogene, we used the fold change value for *Plk* in subsequent analyses. For simplicity, we refer to the human probe sets homologous to the genes differentially expressed between tumor and normal bladder in the rodent as "mouse homologs" and "rat homologs" respectively and collectively as "rodent homologs".

Table 1. Stage and Grade of Human Bladder Cancer Specimens.

Stage	Grade (1–4)	*N*
Normal	n/a	15
Ta	1	1
Ta	2	10
T1	2	3
T2	2	1
T2	3	4
T3	3	6
T3	4	3
T4	2	1
T4	3	9

To examine the importance of individual rodent homologs to transformation (normal *vs* cancer) and progression in humans, we first used Student's *t* test to determine the significance of the difference in expression between normal urothelium and non–muscle-invasive cancer, between normal urothelium and muscle-invasive cancer, between non–muscle-invasive and muscle-invasive cancer, and between normal and cancerous urothelium, for the 53 chips in the human bladder microarray data set. Thus, for every homologous probe set, there were four different *P* values representing the significance level of the aforementioned tests. (We considered genes to be significantly differentially expressed if at least half of their corresponding probe sets are significantly differentially expressed in the same direction, unless there are other probe sets significantly differentially expressed in the opposite direction.) To gain more insight into the meaning of these nominal significance values, we additionally calculated the significance of the difference in expression for the remaining 21,873 probe sets on the HG-U133A chips for the four different comparisons described previously.

To determine whether the rodent homologs were enriched with genes significant to human disease progression, we used two similar statistical techniques. First, we performed a one-sided Kolmogorov–Smirnov (KS) test to compare the *P* value distribution of the homologous probe sets to the *P* value distribution of all 22,215 probe sets found on the 53 HG-U133A chips profiling human bladder cancer tissue. To estimate false discovery rate (FDR) *Q* values for the KS tests, we performed the KS test on 1000 groups of randomly selected probe sets (with the same number of probe sets as in the groups of rodent homologs) to generate a distribution of random KS test *P* values. We then used the R package qvalue to estimate the *Q* value for the KS test involving the rodent homologs, using the 1000 random KS *P* values and the rodent homolog KS *P* value as input. We also used the Gene Set Enrichment Analysis (GSEA) program (version 2.0) [22–24] to test the rodent homologs for enrichment with significantly and differentially expressed probe sets in the 53 human samples categorized as previously mentioned, using the *t* test as the gene-ranking method, without collapsing the data set to gene symbols.

To determine whether the patterns of expression in rodent bladder tumors are more similar to those of invasive or noninvasive human cancers, we calculated human expression fold change values for each non–muscle-invasive or muscle-invasive tumor chip by dividing the expression value of an individual probe set by the average expression of all the normal urothelial chips for that probe set. We then generated a "mouse" or "rat" expression profile by assigning the fold change values (from the rodent normal *vs* tumor comparison) for a particular mouse or rat gene to all human probe sets homologous to that gene. We then performed hierarchical clustering analysis of the "rodent" profile and human tumor profiles. To improve the distinction between the clusters

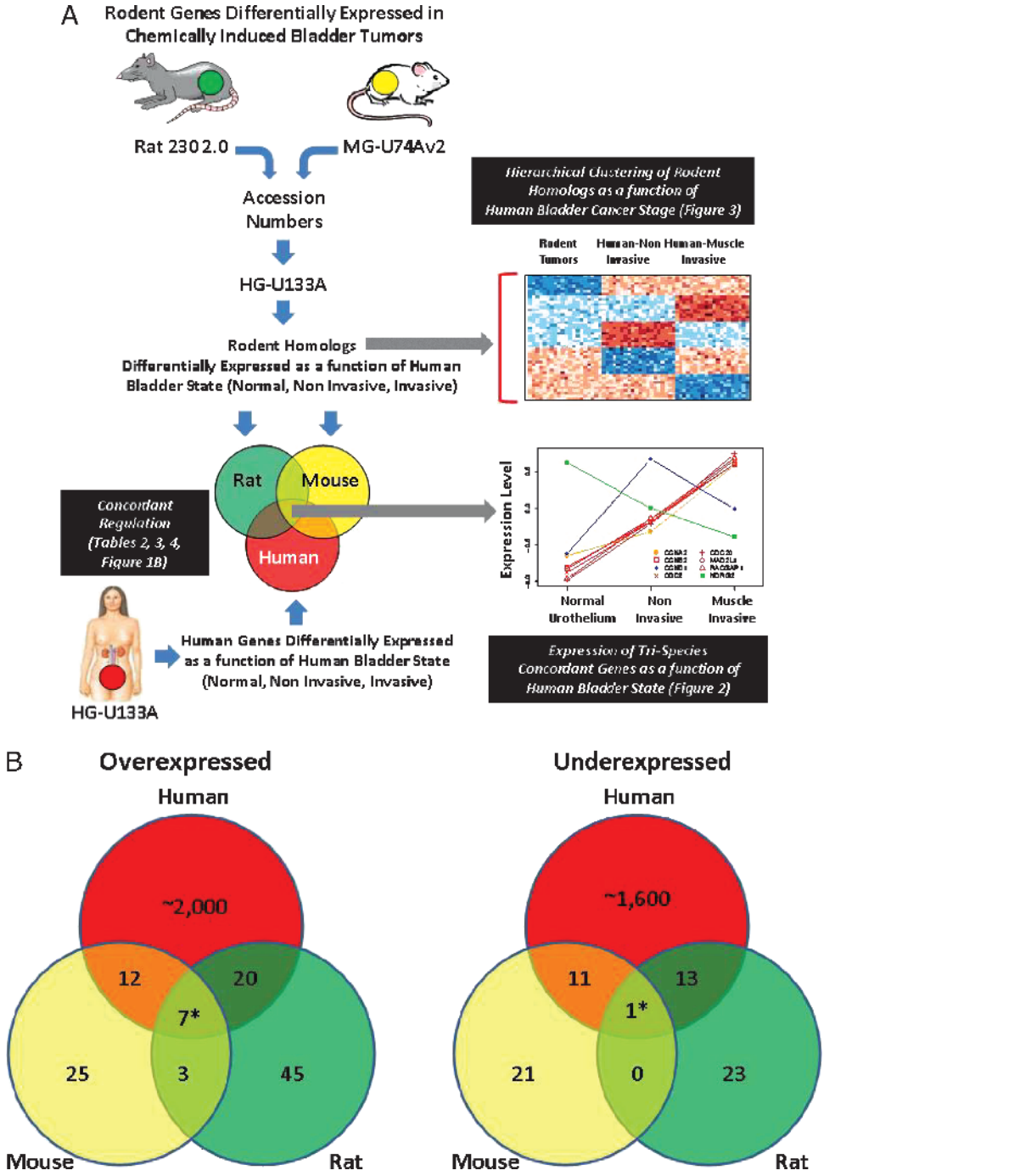

Figure 1. (A) Diagrammatic representation of the analysis workflow and results. (B) Venn diagrams showing the numbers of genes differentially regulated in human, mouse, and rat and concordantly regulated. Shown are genes overexpressed or underexpressed in tumors compared to normal urothelium. Asterisk (*) indicates genes whose pattern of expression is shown in Figure 2.

of non–muscle-invasive and muscle-invasive tumors, we only clustered probe sets with significant ($P < .1$) differences between non–muscle-invasive and muscle-invasive expression.

Results

Evaluation of Rodent Homologs as a Function of Malignancy

We first determined the human homologs of the rodent genes using NetAffx, as described in the Methods section; these are listed in Table W1. We found that the 90 originally published mouse genes correspond to 94 MG-U74Av2 probe sets and that the 145 originally published rat genes correspond to 173 Rat 230 2.0 probe sets. We subsequently found 144 unique human HG-U133A probe sets homologous to the 94 mouse probe sets and 223 unique human HG-U133A probe sets homologous to the 173 rat probe sets. Twenty-five human probe sets were homologous to genes that were differentially expressed in both rat and mouse. We were unable to find human probe sets homologous to nine mouse genes, and as mentioned in the Methods section, we ignored *Plk-ps1* due to its pseudogenous nature; thus, analyses were performed on homologs of 80 mouse genes

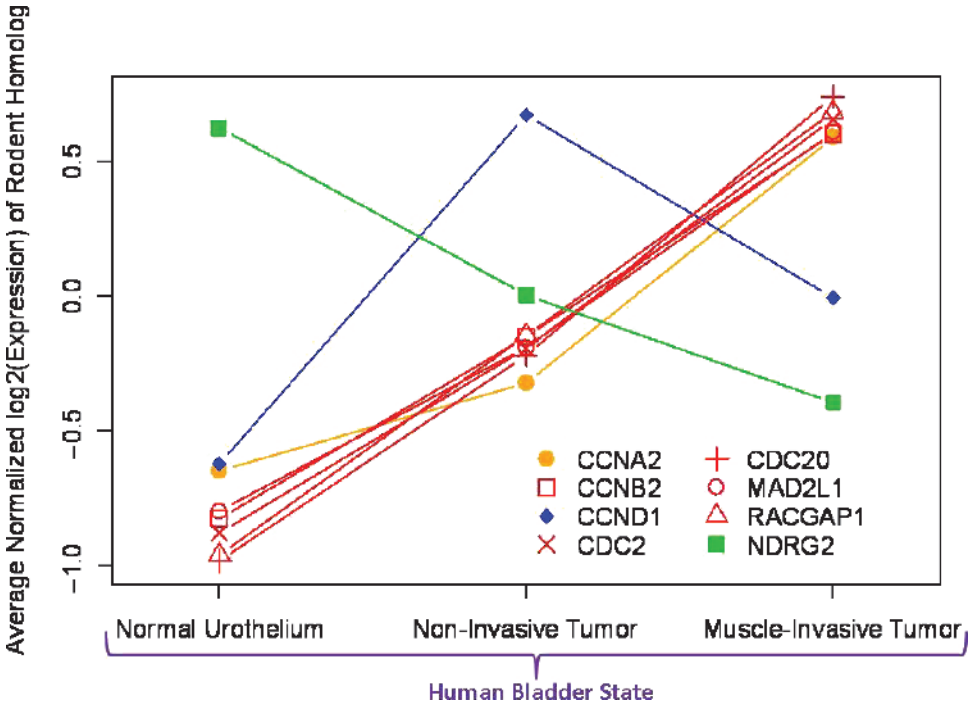

Figure 2. Patterns of expression for genes differentially regulated in human, mouse, and rat bladder tumors as a function of human bladder state. The average normalized log2(gene expression) value for normal urothelium, non–muscle-invasive and muscle-invasive cancers are plotted for each tissue type. Data for all significantly and differentially expressed probe sets for the genes identified with an asterisk (*) in Figure 1*B* are plotted here. Line color codes relate to the gene expression pattern as a function of tumorigenicity and progression as shown in Table 2 (genes in bold). For example, genes with red lines are significantly differentially expressed between normal urothelium and noninvasive tumor and between noninvasive tumor and invasive human tumor.

corresponding to 83 MG-U74Av2 probe sets. Similarly, we were unable to find human probe sets homologous to 35 rat genes; thus, analyses were performed on 110 rat genes corresponding to 138 Rat 230 2.0 probe sets.

We then examined how expression levels of rodent homologs changed according to human bladder state (normal, non–muscle-invasive, and muscle-invasive). After classifying the tissue samples into normal and malignant urothelium, we examined the differential expression between each pair of these three groups of tissues, using Student's *t* test. The numbers of probe sets and corresponding genes that were significantly ($P < .05$) differentially expressed between normal urothelium and urothelial carcinomas were computed. We found that 52 (65%) of 80 mouse homologs [86 (60%) of 144 probe sets] and 71 (63%) of 112 rat homologs [138 (62%) of 223 probe sets] were significantly differentially regulated between human normal urothelium and urothelial carcinoma (of any grade or stage). We further found that of 11 genes homologous among all three species, namely, human, rat, and mouse, 9 genes (82%), or 18 (72%) of 25 probe sets, were similarly differentially expressed.

Identification of Interspecies Concordant Homologs in Transformation and Progression

In Figure 1*B*, we show the numbers of homologous genes that are significantly differentially expressed between normal and cancerous

Table 2. Genes Differentially Regulated with Increasing Invasiveness in Human Bladder Cancer and Concordant in Expression with the Corresponding Rodent Homolog.

Expression Pattern	Mouse Homologs	Rat Homologs
Positively correlated with transformation* and invasiveness	***CCNB2***, ***CDC2***, ***CDC20***, *CKS1B*, ***MAD2L1***, *NMI*, ***RACGAP1***, *RAD51*, *TFDP1*	*BUB1B*, *CCNB1*, ***CCNB2***, ***CDC2***, ***CDC20***, *ECT2*, ***MAD2L1***, ***RACGAP1***
Negatively correlated with transformation invasiveness	N/A	N/A
Significantly increased in cancer, no significant change with invasiveness	*CCNE1*, *PIK3CA*, *RAN*, *RHOG*, *RIN2*	*DUSP6*, *PYCARD*
Significantly decreased in cancer, no significant change with invasiveness	*ARHGDIG*, *GATA4*, *MAP2K6*, *SH3BGR*, *SH3GL2*, *SH3GL3*	*HRASLS*, *LGI1*, *PAK3*, *PPARA*, *WT1*
Significantly increased in non–muscle-invasive disease only	***CCND1***, *MKNK1*, *RAD9A*, *SKAP2*	*AKT1*, *ARHGAP8*, *BCL6*, ***CCND1***, *IGFBP3*, *IGFBP4*, *NDRG4*
Significantly decreased in non–muscle-invasive disease only	*GAS1*	*CARD9*, *CDKN1C*, *FGFR2*, *FRS2*, *NTRK1*, *PDGFRL*, *RASA3*, *RORA*, *SNFT*
Significantly increased in muscle-invasive disease only	***CCNA2***, *CRELD2*, *FOXM1*, *MAP4K4*, *NFKBIE*	***CCNA2***, *CDCA3*, *CDKN2A*, *CDKN2C*, *CDKN3*, *KIF20A*, *MKI67*, *RAP2B*
Significantly decreased in muscle-invasive disease only	*GATA2*, *LMO1*, ***NDRG2***, *SH2B1*, *TCF2*, *TCF21*, *TCF7L1*	*CYP11A1*, *CYP3A43*, *FHIT*, ***NDRG2***, *RAB27B*, *RORC*

Symbols in bold indicate homology with both rat and mouse (eight genes corresponding to the central regions in Figure 1*B* and whose expressions are graphed in Figure 2).
*Defined as the difference between normal and cancer.

Table 3. Gene Ontology of Mouse Homologs Differentially Expressed between Normal Human Urothelium and Cancer, Listed in Table 2.

Classification	Gene
Overexpressed in human muscle-invasive disease	
Cell cycle–related	***CCNA2*** (*Ccna2*), ***CCNB2*** (*Ccnb2*), ***CCND1*** (*Ccnd1*), *CCNE1* (*Ccne1*), ***CDC2*** (*CDC2a*), ***CDC20*** (*CDC20*), *CKS1B* (*Cks1*), ***MAD2L1*** (*Mad2l1*), *TFDP1* (*Dp1*)
EGF/EGFR pathway	*MAP4K4* (*Map4k4*), *PIK3CA* (*Pik3ca*), *SKAP2* (*Scap2*)
Ras pathway	***RACGAP1*** (*Racgap1*), *RAD51* (*Rad51*), *RAD9A* (*Rad9*), *RAN* (*Rasl2–9*), *RHOG* (*Ahrg*), *RIN2* (*Rin2*)
Transcription regulators	*CRELD2* (*Etv6*), *FOXM1* (*Foxm1*), *MKNK1* (*Mknk1*), *NFKBIE* (*Nfkbie*), *NMI* (*Nmi*)
Underexpressed in human muscle-invasive disease	
Cell cycle–related	*GAS1* (*Gas1*)
MAPK/SRC pathway	*MAP2K6* (*Map2k6*), *SH2B1* (*Sh2bpsm1*), *SH3BGR* (*Sh3bgr*), *SH3GL2* (*Sh3gl2*), *SH3GL3* (*Sh3gl3*)
Ras pathway	*ARHGDIG* (*Arhgdig*)
Transcription regulators	*GATA2* (*Gata2*), *GATA4* (*Gata4*), *LMO1* (*Lmo1*), ***NDRG2*** (*Ndr2*), *TCF2* (*Tcf2*), *TCF21* (*Tcf21*), *TCF7L1* (*Tcf3*)

Gene symbols in parentheses represent the homologous mouse gene. Symbols in bold indicate homology with both rat and mouse (eight genes corresponding to the central regions in Figure 1*B* and whose expressions are graphed in Figure 2).

urothelium in all three species. Of 80 human homologs of the genes differentially expressed in mouse tumors, 55 genes were significantly differentially expressed in human ($P < .05$). However, of those 55 genes, only 31 were concordantly regulated; in other words, the direction of the change in expression in bladder tumors was the same in both species. Similarly, of 112 human homologs of the published rat genes, 74 were significantly differentially expressed in humans; 41 of these genes were concordantly regulated in both species. Few genes were differentially expressed and were concordantly regulated in all three species—seven genes were overexpressed and one was repressed. The patterns of gene expression for these eight genes (corresponding to the central regions in Figure 1*B*) are shown in Figure 2. Interestingly, for most of these genes, the expression level is correlated with invasiveness; *NDRG2* is the sole gene to decrease expression with increasing invasiveness. Two genes (*CCNA2* and *CCND1*) are significantly up-regulated only in invasive tumors (compared to noninvasive) and in noninvasive tumors (compared to invasive), respectively.

To better understand the contribution of individual rodent homologs to human disease and progression, a similar analysis was performed for all rodent homologs. A complete list of human genes that are both homologous to and concordantly regulated with either mouse or rat is shown in Table 2. These genes are further classified according to different trends of significant differential expression with invasiveness. In Tables 3 and 4, these genes are listed as a function of the ontologies of the rodent homologs and indicate that genes associated with disease progression are associated with the cell cycle, transcription regulation, or the *Ras* and *EGFR* pathways.

Gene Enrichment Analysis Suggests Rodent Tumors Reflect the Molecular Profile of Human Cancer

To determine whether rodent homologs were significantly enriched with genes significant to human bladder cancer, we performed two separate but similar analyses. First, we applied the KS test to compare the distributions of *t* test *P* values between the rodent homologs and all 22,215 probe sets on the HG-U133A chips. We also used the GSEA program; because the GSEA program does not yet support testing gene sets with both up- and down-regulated genes, we split our gene sets into up- and down-regulated sets and ran the analysis for these split sets. The *P* values and FDR *Q* values for the KS tests and the GSEA tests are listed in Table 5.

The KS test results suggest that although the rodent homologs are not significantly associated with the initial development of human cancer, they are associated with the progression between non–muscle-invasive and muscle-invasive tumors. The results from GSEA tests are more complex: they support the KS test observation that rodent homologs are significantly associated with invasiveness, but the results also suggest that these genes are associated with the development of human tumors. (The small number of genes significantly down-regulated in all species may be the reason the down-regulated sets are not significantly

Table 4. Gene Ontology of Rat Homologs Differentially Expressed between Normal Human Urothelium and Cancer, as Listed in Table 2.

Classification	Gene
Overexpressed in human muscle-invasive disease	
Apoptosis	*PYCARD* (*Pycard*)
Cell cycle–related	***CCNA2*** (*Ccna2*), *CCNB1* (*Ccnb1*), ***CCNB2*** (*Ccnb2*), ***CCND1*** (*Ccnd1*), ***CDC2*** (*Cdc2a*), ***CDC20*** (*Cdc20*), *CDCA3* (*Cdca3*), *CDKN2A* (*Cdkn2a*), *CDKN2C* (*Cdkn2c*), *CDKN3* (*Cdkn3*), *DUSP6* (*Dusp6*), *KIF20A* (*Cdc23*), ***MAD2L1*** (*Mad2l1*), *MKI67* (*Mki67*)
Growth factors	*IGFBP3* (*Igfbp3*), *IGFBP4* (*Igfbp4*)
Oncogenes	*ETC2* (*Etc2*), *NDRG4* (*Ndr4*)
Small G-proteins	***RACGAP1*** (*Racgap1*), *RAP2B* (*Rap2b*)
Underexpressed in human muscle-invasive disease	
Apoptosis	*NTRK1* (*Ntrk1*)
Cell cycle–related	*CDKN1C* (*Cdkn1c*), *PPARA* (*Ppara*), *SNFT* (*Jundp1*)
Growth factors	*FGFR2* (*FGFR2*), *FRS2* (BE112403), *PDGFRL* (BM384311)
Oncogenes	*FHIT* (*Fhit*), *HRASLS* (AI548958), ***NDRG2*** (*Ndrg2*), *PAK3* (*Pak3*), *WT1* (*Wt1*)
Others	*CYP11A1* (*Cyp11a1*), *CYP3A43* (*Cyp3a18*), *LGI1* (*Lgi1*), *RORA* (AI235414), *RORC* (BE110171)
Small G-proteins	*RAB27B* (*Rab27b*), *RASA3* (*Rasa3*)

Gene symbols or accession numbers in parentheses represent the homologous rat gene. Symbols in bold indicate homology with both rat and mouse (eight genes corresponding to the central regions in Figure 1*B* and whose expressions are graphed in Figure 2).

Table 5. Kolmogorov–Smirnov and GSEA *P* values and FDR *Q* values (in Parentheses) Showing the Significance of Enrichment of Sets of Rodent Homologous Genes with Probe Sets Significantly Differentially Expressed in Human Cancer.

		Normal *vs* Cancer		Normal *vs* Non–Muscle-Invasive		Normal *vs* Muscle-Invasive		Noninvasive *vs* Muscle-Invasive	
		KS	GSEA	KS	GSEA	KS	GSEA	KS	GSEA
Mouse	Down	0.323 (0.989)	**0.0383 (0.0713)**	0.254 (1)	**0.0564 (0.109)**	0.151 (0.974)	0.0998 (0.448)	**6×10^{-7} (0.0006)**	**0 (0.00556)**
	Up		**0 (0.0824)**		0.008 (0.312)		**0.0183 (0.0947)**		**0 (0.00972)**
Rat	Down	0.896 (0.976)	**0.0476 (0.0564)**	0.320 (0.999)	**0.0269 (0.0576)**	0.769 (0.947)	0.0646 (0.653)	**5×10^{-4} (0.114)**	**0 (0.00478)**
	Up		**0.00963 (0.0649)**		**0.0463 (0.154)**		**0.00403 (0.0603)**		**0 (0.00321)**
Intersection	Down	0.047 (0.919)	0.278 (0.273)	0.484 (1)	0.285 (0.325)	0.028 (1)	0.372 (0.701)	**2×10^{-4} (0.163)**	0.259 (0.323)
	Up		**0.0286 (0.155)**		0.200 (0.227)		**0.0332 (0.0778)**		**0.042 (0.141)**

Numbers in bold represent statistically significant (FDR < 0.2) results.

enriched.) There are other significant findings as well; in particular, the rat homologs seem to be associated with the initial development of noninvasive human tumors. In general, it is clear that the rodent homologs are indeed relevant to human disease.

Rodent Tumors Have More Molecular Similarity to Invasive Rather Than Noninvasive Human Tumors

To determine whether these rodent models are more relevant for the study of noninvasive or invasive human disease, we performed unsupervised hierarchical clustering of expression fold changes between cancerous and normal tissues for the rodent homologs, where all probe sets homologous to a particular rodent gene are assigned the published fold change values [12,13] or the fold change as a function of tumor stage in the human samples (Table 1). The clusters for the mouse and rat homologs are shown in Figure 3, *A* and *B*, respectively. Figure 3*A* shows that the mouse homologs cluster into two main groups when human tumor stage data are used: one includes a mixture of non–muscle-invasive and muscle-invasive tumors, whereas the other is made up of exclusively muscle-invasive tumors. The "mouse" fold change profile derived from the rodent genes differentially expressed as a function of transformation clusters closely with this latter group, showing that the induced mouse tumors have a similar gene expression to a subset of human invasive tumors. Figure 3*B* shows the "rat" fold change profile clusters with most of the invasive human tumors. Together, these data suggest that rodent bladder tumors have gene expression profiles more similar to those of human invasive than noninvasive tumors and thus would be a better experimental model for the former.

Discussion

We have previously studied genes differentially regulated in metastatic human bladder cancer xenografts in mice to gain insight into regions of the chromosome involved in bladder cancer metastasis [25]. In this article, we study human homologs of rodent genes differentially expressed in chemical-induced animal models of bladder cancer. The comparison of evolutionarily conserved genes in different species is a frequently used technique–sequence alignments and comparative genomics analyses are often used to infer the function or evolutionary origin of a gene or protein, for example. Cross-species comparative expression profiling is relatively new, however, although it seems intuitive that genes with evolutionarily conserved sequences ought to have somewhat similar functions and should presumably be regulated in similar ways. Comparison of the tumor-related expression patterns of homologous genes in animal models of human cancers has been used to study the relevance of liver cancer in zebrafish to human liver [26], to evaluate seven different mouse models of hepatocellular carcinoma to find the most appropriate for liver cancer in humans [27], to compare a transgenic mouse model of lung cancer with a variety of human lung cancers [28], and to analyze several mouse models of breast cancer [29].

In the present study, we examined the patterns of gene expression involved in bladder cancer for three different species. Whereas others have studied a variety of animal models of human cancer [26–29] (including bladder [28]), here we focus on bladder cancer and compare the molecular profiles of carcinogen-induced rodent tumors with that of human disease. The carcinogenesis models are particularly relevant comparators and models because human bladder cancer is often a result of chemical carcinogenesis. Interestingly, we found that a significant proportion of rodent homologs exhibit significant differences in gene expression between non–muscle-invasive and muscle-invasive disease in humans. Furthermore, we determined that the induced rodent tumors exhibit more similarity of gene expression to human muscle-invasive disease than noninvasive disease, which is consistent with their muscle-invasive pathology.

Comparative genomic profiling across species can be divided into two steps: first, one determines whether genes important for a particular condition in one species are important in the other; second, one can determine the degree to which the patterns of gene expression are similar. We found that most human genes homologous to genes differentially expressed (*vs* normal) in bladder tumors in both mouse and rat were also significantly and differentially expressed (*vs* normal) in human tumors, suggesting that these homologous genes are indeed significant to human cancer. To quantify this with more statistical rigor, we performed KS and GSEA tests to examine the enrichment of significantly and differentially expressed genes among rodent homologs. We clearly found that these sets of human homologs were enriched with genes significantly differentially expressed between superficial and muscle-invasive bladder tumors. By focusing on genes that are consistently and concordantly expressed in bladder cancer in three species, we can be confident that such genes are robust candidates for proteins that are biologically important in human bladder carcinogenesis and progression.

Many of the genes differentially expressed between normal urothelium and urothelial cancer in all three species are associated with the cell cycle. For instance, cell division cycle 20 (*CDC20*), cell division cycle 2 (*CDC2*), cyclins D1 and B2 (*CCND1* and *CCNB2*), mitotic arrest–deficient 2, *Saccharomyces cerevisiae*, homolog-like 1 (*MAD2L1*), and cyclin A2 (*CCNA2*) are all associated with progression through the cell cycle. *CDC20* activates the anaphase-promoting complex [30], *CCNB2* activates *CDC2* [31], which promotes entry into metaphase [32,33], *MAD2L1* is involved with the mitotic spindle checkpoint

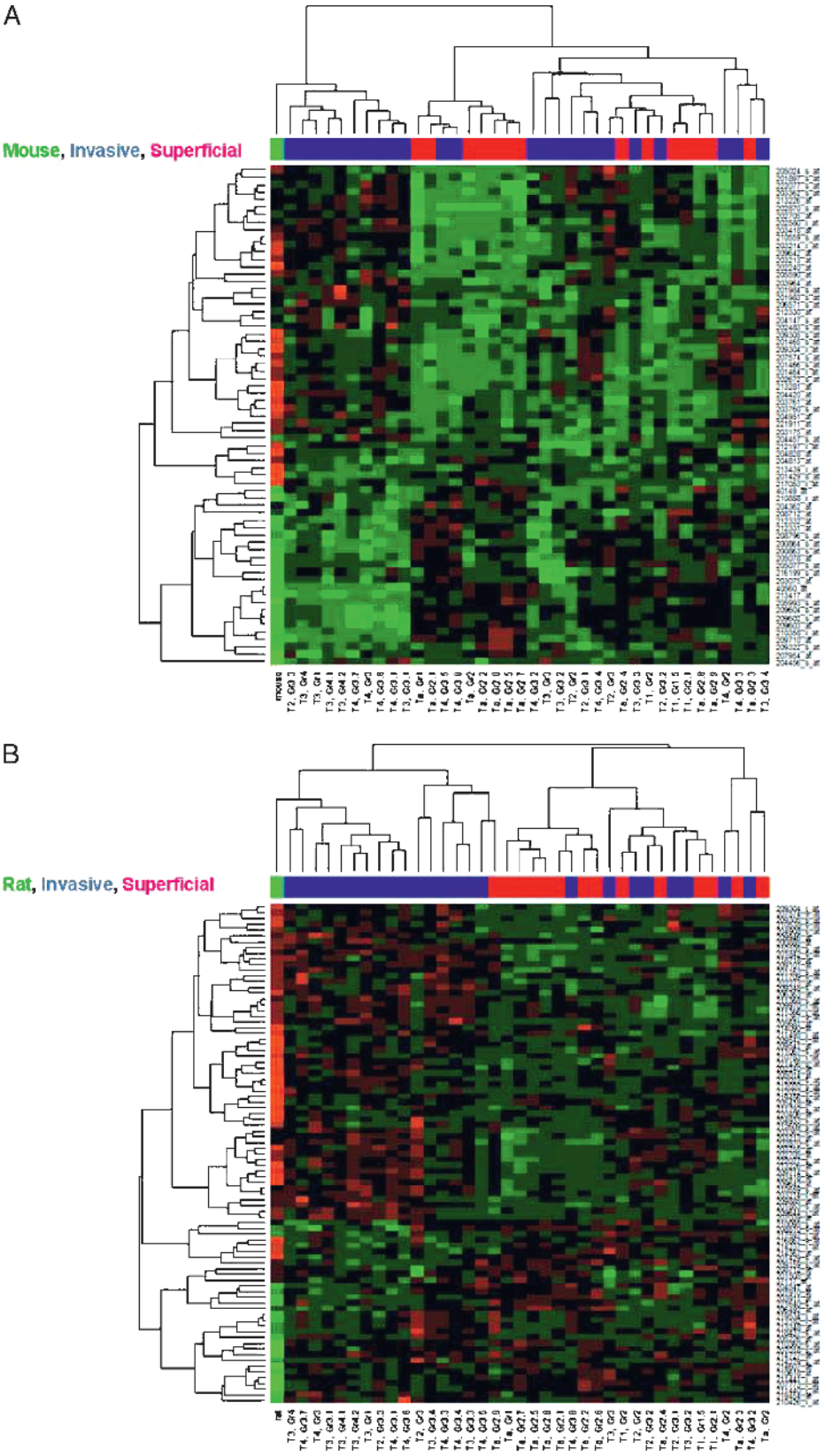

Figure 3. Hierarchical clustering of rodent homologs with human cancer. Fold changes between gene expression values in human non–muscle-invasive and muscle-invasive tumors are hierarchically clustered with "mouse" (A) and "rat" (B) gene expression profiles. The probe sets in the "rodent" gene profiles are assigned published [12,13] fold change values (cancer *vs* normal) corresponding to the homologous rodent genes. Probe sets overexpressed in cancer are colored red, whereas underexpressed probe sets are colored green. HG-U133A probe sets are listed on the right, the stage and grade of the tumors characterized on the chips are shown on the bottom, and the color bar near the top of the figure represents the classification of the tumor: red indicates non–muscle-invasive tumors, blue indicates muscle-invasive tumors, and green indicates the mouse (A) or the rat profile (B).

[34], and *CCNA2* promotes entry into synthesis and metaphase [35]. Other genes differentially expressed in bladder tumors in all three species include RAC GTPase–activating protein 1 (*RACGAP1*), which deactivates RAC proteins and is overexpressed in tumors, and N-*myc* downstream-regulated gene 2 (*NDRG2*), which is underexpressed in tumors. *NDRG2* is a member of the NDRG family, of which *NDRG1* is associated with apoptosis [36]. Furthermore, all, with the exception of *NDRG2*, are differentially expressed between non–muscle-invasive and muscle-invasive human tumors. These genes are overexpressed in muscle-invasive disease, with the exception of *CCND1*, which is underexpressed. Lindgren et al. [37] mentioned that *CDC2*, *CCNB2*, *BUB1*, and *MAD2L1* are in a cell cycle– and mitosis-related cluster of genes, which correlated expression with tumor progression. Blaveri et al. [38] said that *CCNA2* and *CDC2* were more highly expressed in a cluster of high-grade pTa and pT1 tumors than in a cluster of mainly low-grade pTa tumors, suggesting that the tumors in the first cluster were more aggressive. These corroborate our findings that the mouse and rat homologs are indeed important to bladder cancer.

Finally, through unsupervised hierarchical clustering of fold change profiles, we determined that rodent bladder tumors are closely associated with muscle-invasive human tumors. This suggests that such rodent tumors are good models for the mechanistic study of genes putatively involved in invasive and metastatic bladder cancer, especially those that are concordantly expressed in bladder cancer in three species.

In conclusion, this work suggests that carcinogen-induced rodent models of urothelial cancer share genetic similarities with pathways relevant to the development of muscle invasive human disease and provide genes that are candidate drivers or biomarkers of this process.

References

[1] American Cancer Society (2008). *Cancer Facts and Figures 2008.* Atlanta, GA: American Cancer Society.

[2] Stein JP, Lieskovsky G, Cote R, Groshen S, Feng AC, Boyd S, Skinner E, Bochner B, Thangathurai D, Mikhail M, et al. (2001). Radical cystectomy in the treatment of invasive bladder cancer: long-term results in 1,054 patients. *J Clin Oncol* **19**, 666–675.

[3] Howe GR, Burch JD, Miller AB, Cook GM, Esteve J, Morrison B, Gordon P, Chambers LW, Fodor G, and Winsor GM (1980). Tobacco use, occupation, coffee, various nutrients, and bladder cancer. *J Natl Cancer Inst* **64**, 701–713.

[4] Wynder EL and Goldsmith R (1977). The epidemiology of bladder cancer: a second look. *Cancer* **40**, 1246–1268.

[5] Cole P, Hoover R, and Friedell GH (1972). Occupation and cancer of the lower urinary tract. *Cancer* **29**, 1250–1260.

[6] Matanoski GM and Elliott EA (1981). Bladder cancer epidemiology. *Epidemiol Rev* **3**, 203–229.

[7] Grubbs CJ, Lubet RA, Koki AT, Leahy KM, Masferrer JL, Steele VE, Kelloff GJ, Hill DL, and Seibert K (2000). Celecoxib inhibits *N*-butyl-*N*-(4-hydroxybutyl)-nitrosamine-induced urinary bladder cancers in male B6D2F1 mice and female Fischer-344 rats. *Cancer Res* **60**, 5599–5602.

[8] Grubbs CJ, Moon RC, Squire RA, Farrow GM, Stinson SF, Goodman DG, Brown CC, and Sporn MB (1977). 13-*cis*-Retinoic acid: inhibition of bladder carcinogenesis induced in rats by *N*-butyl-*N*-(4-hydroxybutyl)nitrosamine. *Science* **198**, 743–744.

[9] Druckrey H, Preussmann R, Ivankovic S, Schmidt CH, Mennel HD, and Stahl KW (1964). Selective induction of bladder cancer in rats by dibutyl- and *N*-butyl-*N*-butanol(4)-nitrosamine. *Z Krebsforsch* **66**, 280–290.

[10] Fukushima S, Hirose M, Tsuda H, Shirai T, and Hirao K (1976). Histological classification of urinary bladder cancers in rats induced by *N*-butyl-*n*-(4-hydroxybutyl)nitrosamine. *Gann* **67**, 81–90.

[11] Kunze E, Schauer A, and Schatt S (1976). Stages of transformation in the development of *N*-butyl-*N*-(4-hydroxybutyl)-nitrosamine–induced transitional cell carcinomas in the urinary bladder of rats. *Z Krebsforsch Klin Onkol Cancer Res Clin Oncol* **87**, 139–160.

[12] Yao R, Lemon WJ, Wang Y, Grubbs CJ, Lubet RA, and You M (2004). Altered gene expression profile in mouse bladder cancers induced by hydroxybutyl(butyl) nitrosamine. *Neoplasia* **6**, 569–577.

[13] Yao R, Yi Y, Grubbs CJ, Lubet RA, and You M (2007). Gene expression profiling of chemically induced rat bladder tumors. *Neoplasia* **9**, 207–221.

[14] Barrett T, Troup DB, Wilhite SE, Ledoux P, Rudnev D, Evangelista C, Kim IF, Soboleva A, Tomashevsky M, and Edgar R (2007). NCBI GEO: mining tens of millions of expression profiles—database and tools update. *Nucleic Acids Res* **35**, D760–D765.

[15] Dyrskjøt L, Kruhøffer M, Thykjaer T, Marcussen N, Jensen JL, Møller K, and Ørntoft TF (2004). Gene expression in the urinary bladder: a common carcinoma *in situ* gene expression signature exists disregarding histopathological classification. *Cancer Res* **64**, 4040–4048.

[16] Edgar R, Domrachev M, and Lash AE (2002). Gene Expression Omnibus: NCBI gene expression and hybridization array data repository. *Nucleic Acids Res* **30**, 207–210.

[17] Smith SC, Oxford G, Baras AS, Owens C, Havaleshko D, Brautigan DL, Safo MK, and Theodorescu D (2007). Expression of ral GTPases, their effectors, and activators in human bladder cancer. *Clin Cancer Res* **13**, 3803–3813.

[18] Bolstad BM, Irizarry RA, Astrand M, and Speed TP (2003). A comparison of normalization methods for high density oligonucleotide array data based on variance and bias. *Bioinformatics* **19**, 185–193.

[19] Irizarry RA, Bolstad BM, Collin F, Cope LM, Hobbs B, and Speed TP (2003). Summaries of Affymetrix GeneChip probe level data. *Nucleic Acids Res* **31**, e15.

[20] Irizarry RA, Hobbs B, Collin F, Beazer-Barclay YD, Antonellis KJ, Scherf U, and Speed TP (2003). Exploration, normalization, and summaries of high density oligonucleotide array probe level data. *Biostatistics* **4**, 249–264.

[21] Liu G, Loraine AE, Shigeta R, Cline M, Cheng J, Valmeekam V, Sun S, Kulp D, and Siani-Rose MA (2003). NetAffx: Affymetrix probesets and annotations. *Nucleic Acids Res* **31**, 82–86.

[22] Mootha VK, Lindgren CM, Eriksson KF, Subramanian A, Sihag S, Lehar J, Puigserver P, Carlsson E, Ridderstrale M, Laurila E, et al. (2003). PGC-1α–responsive genes involved in oxidative phosphorylation are coordinately downregulated in human diabetes. *Nat Genet* **34**, 267–273.

[23] Subramanian A, Kuehn H, Gould J, Tamayo P, and Mesirov JP (2007). GSEA-P: a desktop application for Gene Set Enrichment Analysis. *Bioinformatics* **23**, 3251–3253.

[24] Subramanian A, Tamayo P, Mootha VK, Mukherjee S, Ebert BL, Gillette MA, Paulovich A, Pomeroy SL, Golub TR, Lander ES, et al. (2005). Gene set enrichment analysis: a knowledge-based approach for interpreting genome-wide expression profiles. *Proc Natl Acad Sci USA* **102**, 15545–15550.

[25] Wu Z, Siadaty MS, Riddick G, Frierson HF Jr, Lee JK, Golden W, Knuutila S, Hampton GM, El-Rifai W, and Theodorescu D (2006). A novel method for gene expression mapping of metastatic competence in human bladder cancer. *Neoplasia* **8**, 181–189.

[26] Lam SH, Wu YL, Vega VB, Miller LD, Spitsbergen J, Tong Y, Zhan H, Govindarajan KR, Lee S, Mathavan S, et al. (2006). Conservation of gene expression signatures between zebrafish and human liver tumors and tumor progression. *Nat Biotechnol* **24**, 73–75.

[27] Lee JS, Chu IS, Mikaelyan A, Calvisi DF, Heo J, Reddy JK, and Thorgeirsson SS (2004). Application of comparative functional genomics to identify best-fit mouse models to study human cancer. *Nat Genet* **36**, 1306–1311.

[28] Sweet-Cordero A, Mukherjee S, Subramanian A, You H, Roix JJ, Ladd-Acosta C, Mesirov J, Golub TR, and Jacks T (2005). An oncogenic KRAS2 expression signature identified by cross-species gene-expression analysis. *Nat Genet* **37**, 48–55.

[29] Herschkowitz JI, Simin K, Weigman VJ, Mikaelian I, Usary J, Hu Z, Rasmussen KE, Jones LP, Assefnia S, Chandrasekharan S, et al. (2007). Identification of conserved gene expression features between murine mammary carcinoma models and human breast tumors. *Genome Biol* **8**, R76.

[30] Fang G, Yu H, and Kirschner MW (1998). Direct binding of CDC20 protein family members activates the anaphase-promoting complex in mitosis and G_1. *Mol Cell* **2**, 163–171.

[31] Labbe JC, Capony JP, Caput D, Cavadore JC, Derancourt J, Kaghad M, Lelias JM, Picard A, and Doree M (1989). MPF from starfish oocytes at first meiotic metaphase is a heterodimer containing one molecule of cdc2 and one molecule of cyclin B. *EMBO J* **8**, 3053–3058.

[32] Nurse P and Bissett Y (1981). Gene required in G_1 for commitment to cell cycle and in G_2 for control of mitosis in fission yeast. *Nature* **292**, 558–560.

[33] Nurse P and Thuriaux P (1980). Regulatory genes controlling mitosis in the fission yeast *Schizosaccharomyces pombe*. *Genetics* **96**, 627–637.

[34] Li Y and Benezra R (1996). Identification of a human mitotic checkpoint gene: *hsMAD2*. *Science* **274**, 246–248.

[35] Pagano M, Pepperkok R, Verde F, Ansorge W, and Draetta G (1992). Cyclin A is required at two points in the human cell cycle. *EMBO J* **11**, 961–971.

[36] Kalaydjieva L, Gresham D, Gooding R, Heather L, Baas F, de Jonge R, Blechschmidt K, Angelicheva D, Chandler D, Worsley P, et al. (2000). N-*myc* downstream-regulated gene 1 is mutated in hereditary motor and sensory neuropathy-Lom. *Am J Hum Genet* **67**, 47–58.

[37] Lindgren D, Liedberg F, Andersson A, Chebil G, Gudjonsson S, Borg A, Mansson W, Fioretos T, and Hoglund M (2006). Molecular characterization of early-stage bladder carcinomas by expression profiles, FGFR3 mutation status, and loss of 9q. *Oncogene* **25**, 2685–2696.

[38] Blaveri E, Simko JP, Korkola JE, Brewer JL, Baehner F, Mehta K, Devries S, Koppie T, Pejavar S, Carroll P, et al. (2005). Bladder cancer outcome and subtype classification by gene expression. *Clin Cancer Res* **11**, 4044–4055.

Table W1. Rodent Accession Numbers and/or Gene Symbols with Their Corresponding Affymetrix Mouse MG-74Av2 or Rat 230 2.0 Probe Sets, Matched with Their Orthologous Human HG-U133A Probe Sets and Corresponding Human Gene Symbols.

Mouse Accession Number	Mouse Gene Symbol	Mouse MG-74Av2 Probe Set	Human HG-U133A Probe Set	Human Gene Symbol
U73198	*Arhgdig*	102677_at	206888_s_at	*ARHGDIG*
U58203	*Arhgef1*	98001_at	203055_s_at	*ARHGEF1*
U19118	*Atf3*	104155_f_at	202672_s_at	*ATF3*
U43678	*Atm*	101180_at	210858_x_at	*ATM*
U43678	*Atm*	101180_at	208442_s_at	*ATM*
U43678	*Atm*	101180_at	212672_at	*ATM*
AF002823	*Bub1*	104097_at	209642_at	*BUB1*
AF002823	*Bub1*	104097_at	216277_at	*BUB1*
AF002823	*Bub1*	104097_at	216275_at	*BUB1*
AF002823	*Bub1*	104097_at	215509_s_at	*BUB1*
AF002823	*Bub1*	104097_at	215508_at	*BUB1*
X75483	*Ccna2*	99186_at	213226_at	*CCNA2*
X75483	*Ccna2*	99186_at	203418_at	*CCNA2*
X66032	*Ccnb2*	94294_at	202705_at	*CCNB2*
AI849928	*Ccnd1*	94232_at	208712_at	*CCND1*
AI849928	*Ccnd1*	94232_at	208711_s_at	*CCND1*
X75888	*Ccne1*	103034_at	213523_at	*CCNE1*
L49507	*Ccng1*	160127_at	208796_s_at	*CCNG1*
M38724	*CDC2a*	100128_at	203213_at	*CDC2*
M38724	*CDC2a*	100128_at	210559_s_at	*CDC2*
M38724	*CDC2a*	100128_at	203214_x_at	*CDC2*
AW061324	*CDC20*	96319_at	202870_s_at	*CDC20*
L16926	*CDC25c*	102934_s_at	205167_s_at	*CDC25C*
L16926	*CDC25c*	102934_s_at	217010_s_at	*CDC25C*
L16926	*CDC25c*	102934_s_at	216914_at	*CDC25C*
AB025409	*Cks1*	97468_at	201897_s_at	*CKS1B*
AF005423	*Clk4*	101937_s_at	210346_s_at	*CLK4*
AI845538	*Etv6*	160119_at	218358_at	*CRELD2*
AW049716	*Egfr*	101842_g_at	201983_s_at	*EGFR*
AW049716	*Egfr*	101842_g_at	201984_s_at	*EGFR*
AW049716	*Egfr*	101842_g_at	211607_x_at	*EGFR*
AW049716	*Egfr*	101842_g_at	210984_x_at	*EGFR*
AW049716	*Egfr*	101842_g_at	211551_at	*EGFR*
AW049716	*Egfr*	101842_g_at	211550_at	*EGFR*
AI844939	*Cri1*	99191_at	211698_at	*EID1*
AI844939	*Cri1*	99191_at	208669_s_at	*EID1*
AI844939	*Cri1*	99191_at	208670_s_at	*EID1*
Z36885	*Elk4*	98732_at	206919_at	*ELK4*
Z36885	*Elk4*	98732_at	205994_at	*ELK4*
L10426	*Etv1*	92927_at	221911_at	*ETV1*
L10426	*Etv1*	92927_at	206501_x_at	*ETV1*
L10426	*Etv1*	92927_at	217061_s_at	*ETV1*
L10426	*Etv1*	92927_at	217053_x_at	*ETV1*
X63190	*Etv4*	92979_at	211603_s_at	*ETV4*
AF017128	*Fosl1*	99835_at	204420_at	*FOSL1*
AV251191	*Foxc2*	162016_f_at	214520_at	*FOXC2*
Y11245	*Foxm1*	98306_g_at	202580_x_at	*FOXM1*
AV138783	*Gadd45b*	161666_f_at	207574_s_at	*GADD45B*
AV138783	*Gadd45b*	161666_f_at	209305_s_at	*GADD45B*
AV138783	*Gadd45b*	161666_f_at	209304_x_at	*GADD45B*
AV138783	*Gadd45b*	161666_f_at	213560_at	*GADD45B*
X65128	*Gas1*	94813_at	204456_s_at	*GAS1*
X65128	*Gas1*	94813_at	204457_s_at	*GAS1*
AB000096	*Gata2*	102789_at	209710_at	*GATA2*
AB000096	*Gata2*	102789_at	210358_x_at	*GATA2*
AB000096	*Gata2*	102789_at	207954_at	*GATA2*
X55123	*Gata3*	100924_at	209602_s_at	*GATA3*
X55123	*Gata3*	100924_at	209603_at	*GATA3*
X55123	*Gata3*	100924_at	209604_s_at	*GATA3*
M98339	*Gata4*	102713_at	205517_at	*GATA4*
X12761	*Jun*	100130_at	201464_x_at	*JUN*
X12761	*Jun*	100130_at	201466_s_at	*JUN*
X12761	*Jun*	100130_at	201465_s_at	*JUN*
X12761	*Jun*	100130_at	213281_at	*JUN*
AW122780	*Lasp1*	93793_at	200618_at	*LASP1*
AW124311	*Lmo1*	102413_at	206718_at	*LMO1*
AF074600	*Lmo4*	98122_at	209205_s_at	*LMO4*
AF074600	*Lmo4*	98122_at	209204_at	*LMO4*
U83902	*Mad2l1*	99632_at	203362_s_at	*MAD2L1*
U39066	*Map2k6*	102828_at	205698_s_at	*MAP2K6*
U39066	*Map2k6*	102828_at	205699_at	*MAP2K6*
AV270901	*Map3k4*	161568_f_at	216199_s_at	*MAP3K4*

Table W1. (*continued*)

Mouse Accession Number	Mouse Gene Symbol	Mouse MG-74Av2 Probe Set	Human HG-U133A Probe Set	Human Gene Symbol
AV270901	*Map3k4*	161568_f_at	204089_x_at	*MAP3K4*
AV341985	*Map3k8*	161768_r_at	205027_s_at	*MAP3K8*
U88984	*Map4k4*	102195_at	206571_s_at	*MAP4K4*
U88984	*Map4k4*	102195_at	218181_s_at	*MAP4K4*
D87271	*Erk2*	93253_at	212271_at	*MAPK1*
D87271	*Erk2*	93253_at	208351_s_at	*MAPK1*
L35236	*Mapk10*	100470_at	204813_at	*MAPK10*
Y11091	*Mknk1*	92464_at	209467_s_at	*MKNK1*
AV277546	*Rhoip3*	162066_f_at	212197_x_at	*M-RIP*
AV277546	*Rhoip3*	162066_f_at	214771_x_at	*M-RIP*
AV277546	*Rhoip3*	162066_f_at	214694_at	*M-RIP*
AB033921	*Ndr2*	96088_at	214279_s_at	*NDRG2*
AB033921	*Ndr2*	96088_at	214278_s_at	*NDRG2*
AB033921	*Ndr2*	96088_at	206453_s_at	*NDRG2*
M57999	*Nfkb1*	98427_s_at	209239_at	*NFKB1*
AF030896	*Nfkbie*	101727_at	203927_at	*NFKBIE*
AF019249	*Nmi*	101424_at	203964_at	*NMI*
D50264	*Arhq*	101466_at	205077_s_at	*PIGF*
D50264	*Arhq*	101466_at	205078_at	*PIGF*
U52193	*Pik3c2a*	92311_s_at	213070_at	*PIK3C2A*
U03279	*Pik3ca*	92452_at	204369_at	*PIK3CA*
U01063	*Plk*	93099_f_at	202240_at	*PLK1*
U01063	*Plk*	93099_f_at	201429_s_at	*PLK1* (*RPL37A*)
AI853996	*Rab11a*	96238_at	200863_s_at	*RAB11A*
AI853996	*Rab11a*	96238_at	200864_s_at	*RAB11A*
AW208630	*Rab33b*	97058_f_at	221014_s_at	*RAB33B*
AB027290	*Rab9*	95516_at	221808_at	*RAB9A*
AA967636	*Rac3*	104180_at	206103_at	*RAC3*
AW122347	*Racgap1*	94953_at	222077_s_at	*RACGAP1*
D13803	*Rad51*	104527_at	205024_s_at	*RAD51*
D13803	*Rad51*	104527_at	205023_at	*RAD51*
AF045663	*Rad9*	93522_at	204828_at	*RAD9A*
L32752	*Rasl2-9*	102821_s_at	200750_s_at	*RAN*
L32752	*Rasl2-9*	102821_s_at	200749_at	*RAN*
X56045	*Ranbp1*	98573_r_at	202483_s_at	*RANBP1*
X56045	*Ranbp1*	98573_r_at	202482_x_at	*RANBP1*
X56045	*Ranbp1*	98573_r_at	221915_s_at	*RANBP1*
AF106070	*Rasgrp1*	98307_at	205590_at	*RASGRP1*
U35142	*Rbbp7*	93081_at	201092_at	*RBBP7*
U36799	*Rbl2*	95617_at	212332_at	*RBL2*
U36799	*Rbl2*	95617_at	212331_at	*RBL2*
X99963	*Rhob*	101030_at	212099_at	*RHOB*
AB025943	*Ahrg*	97927_at	203175_at	*RHOG*
AA739233	*Ahrh*	103231_at	204951_at	*RHOH*
AI835968	*Rin2*	160827_at	209684_at	*RIN2*
U73941	*Rap2ip*	103960_at	206196_s_at	*RPIP8*
U73941	*Rap2ip*	103960_at	213439_x_at	*RPIP8*
AF020526	*Sh2bpsm1*	101843_at	40149_at	*SH2B1*
AF020526	*Sh2bpsm1*	101843_at	209322_s_at	*SH2B1*
AW048272	*Sh3bgr*	96205_at	204979_s_at	*SH3BGR*
X87671	*Sh3bp1*	92666_at	213633_at	*SH3BP1*
U58886	*Sh3gl2*	92673_at	205751_at	*SH3GL2*
U58887	*Sh3gl3*	101412_at	205637_s_at	*SH3GL3*
U58887	*Sh3gl3*	101412_at	205636_at	*SH3GL3*
U58887	*Sh3gl3*	101412_at	211565_at	*SH3GL3*
AB014485	*Scap2*	102012_at	204362_at	*SKAP2*
AB014485	*Scap2*	102012_at	216899_s_at	*SKAP2*
AB014485	*Scap2*	102012_at	204361_s_at	*SKAP2*
U29056	*Sla*	99876_at	203761_at	*SLA*
U29056	*Sla*	99876_at	203760_s_at	*SLA*
U60530	*Madh2*	104536_at	203077_s_at	*SMAD2*
U60530	*Madh2*	104536_at	203075_at	*SMAD2*
U60530	*Madh2*	104536_at	203076_s_at	*SMAD2*
U15566	*Tbx2*	92705_at	40560_at	*TBX2*
U15566	*Tbx2*	92705_at	213417_at	*TBX2*
U15566	*Tbx2*	92705_at	205993_s_at	*TBX2*
AB008174	*Tcf2*	101396_at	208135_at	*TCF2*
AB008174	*Tcf2*	101396_at	205313_at	*TCF2*
AF035717	*Tcf21*	103050_at	204931_at	*TCF21*
AJ223069	*Tcf3*	160780_at	221016_s_at	*TCF7L1*
AF043939	*Dp1*	97565_r_at	212330_at	*TFDP1*
AF043939	*Dp1*	97565_r_at	204147_s_at	*TFDP1*

Table W1. (*continued*)

Rat Accession Number	Rat Gene Symbol	Rat 230 2.0 Probe Set	Human HG-U133A Probe Set	Human Gene Symbol
NM_033230	*Akt1*	1383126_at	207163_s_at	*AKT1*
NM_031575	*Akt3*	1387592_at	219393_s_at	*AKT3*
NM_031575	*Akt3*	1387592_at	212609_s_at	*AKT3*
NM_031575	*Akt3*	1387592_at	212607_at	*AKT3*
BE111827	*Arhgap4*	1374735_at	204425_at	*ARHGAP4*
AA945062	*Arhgap8*	1376501_at	37117_at	*ARHGAP8*
AA945062	*Arhgap8*	1376501_at	205980_s_at	*PRR5*
BF285771	*Arhgdib*	1373881_at	201288_at	*ARHGDIB*
BG377320		1373541_at	203756_at	*ARHGEF17*
BE116855	*Bcl11b*	1384944_at	219528_s_at	*BCL11B*
NM_133416	*Bcl2a1*	1368482_at	205681_at	*BCL2A1*
AI411774	*Bcl3*	1398482_at	204908_s_at	*BCL3*
AI411774	*Bcl3*	1398482_at	204907_s_at	*BCL3*
AI237606	*Bcl6*	1379368_at	203140_at	*BCL6*
AI237606	*Bcl6*	1379368_at	215990_s_at	*BCL6*
NM_023987	*Birc2*	1370113_at	210538_s_at	*BIRC3*
AI227742	*Bok*	1373733_at	221454_at	*BOK*
BF396613	*Brca2*	1381141_at	208368_s_at	*BRCA2*
BF396613	*Brca2*	1381141_at	214727_at	*BRCA2*
BF388785	*Bub1*	1385086_at	209642_at	*BUB1*
BF388785	*Bub1*	1385086_at	216277_at	*BUB1*
BF388785	*Bub1*	1385086_at	216275_at	*BUB1*
BF388785	*Bub1*	1385086_at	215509_s_at	*BUB1*
BF388785	*Bub1*	1385086_at	215508_at	*BUB1*
BF557145	*Bub1b*	1383926_at	203755_at	*BUB1B*
NM_022303	*LOC64171*	1368637_at	220162_s_at	*CARD9*
BI303370	*Rad51*	1395480_at	220247_at	*CASC5*
D85899	*Casp1*	1369186_at	211368_s_at	*CASP1*
D85899	*Casp1*	1369186_at	211367_s_at	*CASP1*
D85899	*Casp1*	1369186_at	211366_x_at	*CASP1*
D85899	*Casp1*	1369186_at	209970_x_at	*CASP1*
D85899	*Casp1*	1369186_at	206011_at	*CASP1*
NM_053736	*Casp11*	1387818_at	209310_s_at	*CASP4*
NM_053736	*Casp11*	1387818_at	213596_at	*CASP4*
NM_053736	*Casp11*	1387818_at	208340_at	*CASP4*
AA998516	*Ccna2*	1379582_a_at	213226_at	*CCNA2*
AA998516	*Ccna2*	1379582_a_at	203418_at	*CCNA2*
X64589	*Ccnb1*	1370346_at	214710_s_at	*CCNB1*
AW253821	*Ccnb2*	1389566_at	202705_at	*CCNB2*
X75207	*Ccnd1*	1371150_at	208712_at	*CCND1*
X75207	*Ccnd1*	1371150_at	208711_s_at	*CCND1*
NM_019296	*Cdc2a*	1367776_at	203213_at	*CDC2*
NM_019296	*Cdc2a*	1367776_at	210559_s_at	*CDC2*
NM_019296	*Cdc2a*	1367776_at	203214_x_at	*CDC2*
U05341	*Cdc20*	1387895_s_at	202870_s_at	*CDC20*
NM_133572	*Cdc25B*	1370034_at	201853_s_at	*CDC25B*
BF417638	*Cdca3*	1374449_at	221436_s_at	*CDCA3*
AI013919	*Cdkn1c*	1372299_at	219533_at	*CDKN1C*
AI013919	*Cdkn1c*	1372299_at	213183_s_at	*CDKN1C*
AI013919	*Cdkn1c*	1372299_at	216894_x_at	*CDKN1C*
AI013919	*Cdkn1c*	1372299_at	213182_x_at	*CDKN1C*
AI013919	*Cdkn1c*	1372299_at	219534_x_at	*CDKN1C*
AI013919	*Cdkn1c*	1372299_at	213348_at	*CDKN1C*
AF474976	*Cdkn2a*	1369194_a_at	209644_x_at	*CDKN2A*
AF474976	*Cdkn2a*	1369194_a_at	207039_at	*CDKN2A*
AF474976	*Cdkn2a*	1369194_a_at	211156_at	*CDKN2A*
NM_131902	*Cdkn2c*	1370054_at	204159_at	*CDKN2C*
NM_131902	*Cdkn2c*	1370054_at	211792_s_at	*CDKN2C*
BE113362	*Cdkn3*	1372685_at	209714_s_at	*CDKN3*
AI576758	*Scgf*	1392672_at	211709_s_at	*CLEC11A*
AI576758	*Scgf*	1392672_at	210783_x_at	*CLEC11A*
AI576758	*Scgf*	1392672_at	205131_x_at	*CLEC11A*
BG371721	*Clpx*	1398698_at	204809_at	*CLPX*
BE107780		1398204_at	203575_at	*CSNK2A2*
NM_022266	*Ctgf*	1367631_at	209101_at	*CTGF*
NM_017286	*Cyp11a1*	1368468_at	204309_at	*CYP11A1*
X00469	*Cyp1a1*	1370269_at	205749_at	*CYP1A1*
D38381	*Cyp3a18*	1398307_at	211442_x_at	*CYP3A43*
D38381	*Cyp3a18*	1398307_at	211440_x_at	*CYP3A43*
D38381	*Cyp3a18*	1398307_at	207773_x_at	*CYP3A43*
D38381	*Cyp3a18*	1398307_at	211441_x_at	*CYP3A43*
NM_053679	*Dffa*	1389195_at	203277_at	*DFFA*

Table W1. (*continued*)

Rat Accession Number	Rat Gene Symbol	Rat 230 2.0 Probe Set	Human HG-U133A Probe Set	Human Gene Symbol
NM_053883	*Dusp6*	1387024_at	208892_s_at	*DUSP6*
NM_053883	*Dusp6*	1387024_at	208891_at	*DUSP6*
NM_053883	*Dusp6*	1387024_at	208893_s_at	*DUSP6*
AI578135	*Ect2*	1383747_at	219787_s_at	*ECT2*
BF284634		1390112_at	201842_s_at	*EFEMP1*
BF284634		1390112_at	201843_s_at	*EFEMP1*
BF418373		1393335_at	219454_at	*EGFL6*
AI547942		1378721_at	201911_s_at	*FARP1*
AI547942		1378721_at	201910_at	*FARP1*
BI289400	*Fes*	1380621_at	205418_at	*FES*
NM_053428	*Fgf13*	1368114_at	205110_s_at	*FGF13*
NM_022603	*Fgfbp1*	1368349_at	205014_at	*FGFBP1*
L19107	*FGFR2*	1388168_a_at	208229_at	*FGFR2*
L19107	*FGFR2*	1388168_a_at	208228_s_at	*FGFR2*
L19107	*FGFR2*	1388168_a_at	211399_at	*FGFR2*
L19107	*FGFR2*	1388168_a_at	211401_s_at	*FGFR2*
L19107	*FGFR2*	1388168_a_at	211398_at	*FGFR2*
L19107	*FGFR2*	1388168_a_at	203639_s_at	*FGFR2*
L19107	*FGFR2*	1388168_a_at	203638_s_at	*FGFR2*
L19107	*FGFR2*	1388168_a_at	208234_x_at	*FGFR2*
L19107	*FGFR2*	1388168_a_at	208225_at	*FGFR2*
L19107	*FGFR2*	1388168_a_at	211400_at	*FGFR2*
NM_021774	*Fhit*	1369318_at	206492_at	*FHIT*
BE112403		1397648_at	221308_at	*FRS2*
AI230396	*Fyn*	1373683_at	216033_s_at	*FYN*
AI230396	*Fyn*	1373683_at	210105_s_at	*FYN*
AI230396	*Fyn*	1373683_at	212486_s_at	*FYN*
BI287978	*Gadd45b*	1372016_at	207574_s_at	*GADD45B*
BI287978	*Gadd45b*	1372016_at	209305_s_at	*GADD45B*
BI287978	*Gadd45b*	1372016_at	209304_x_at	*GADD45B*
BI287978	*Gadd45b*	1372016_at	213560_at	*GADD45B*
AI599423	*Gadd45g*	1388792_at	204121_at	*GADD45G*
NM_017195	*Gap43*	1371287_at	216963_s_at	*GAP43*
NM_017195	*Gap43*	1371287_at	204471_at	*GAP43*
NM_017195	*Gap43*	1371287_at	216967_at	*GAP43*
AJ131902	*Gas7*	1370963_at	210872_x_at	*GAS7*
AJ131902	*Gas7*	1370963_at	211067_s_at	*GAS7*
AJ131902	*Gas7*	1370963_at	202191_s_at	*GAS7*
AJ131902	*Gas7*	1370963_at	207704_s_at	*GAS7*
AJ131902	*Gas7*	1370963_at	202192_s_at	*GAS7*
BI289525	*Gdf1*	1377506_at	206397_x_at	*GDF1*
NM_017017	*Hgf*	1387701_at	210998_s_at	*HGF*
NM_017017	*Hgf*	1387701_at	210997_at	*HGF*
NM_017017	*Hgf*	1387701_at	210755_at	*HGF*
NM_017017	*Hgf*	1387701_at	209960_at	*HGF*
NM_017017	*Hgf*	1387701_at	209961_s_at	*HGF*
BE119649	*Hgfac*	1381006_at	207027_at	*HGFAC*
AI548958		1393790_at	219983_at	*HRASLS*
AI548958		1393790_at	219984_s_at	*HRASLS*
M15481	*Igf1*	1370333_a_at	209540_at	*IGF1*
M15481	*Igf1*	1370333_a_at	209541_at	*IGF1*
M15481	*Igf1*	1370333_a_at	211577_s_at	*IGF1*
M15481	*Igf1*	1370333_a_at	209542_x_at	*IGF1*
NM_012588	*Igfbp3*	1367652_at	210095_s_at	*IGFBP3*
NM_012588	*Igfbp3*	1367652_at	212143_s_at	*IGFBP3*
BE108969	*Igfbp4*	1371462_at	201508_at	*IGFBP4*
AI233246	*Igfbp7*	1371357_at	201163_s_at	*IGFBP7*
AI233246	*Igfbp7*	1371357_at	213910_at	*IGFBP7*
AI233246	*Igfbp7*	1371357_at	201162_at	*IGFBP7*
BE111697	*Cdc23*	1373722_at	218755_at	*KIF20A*
BG381002	*Lcmt1*	1388747_at	221515_s_at	*LCMT1*
AI229354	*Lgi1*	1386023_at	206349_at	*LGI1*
BF412229		1398569_at	221640_s_at	*LRDD*
AI716087		1375894_at	218437_s_at	*LZTFL1*
AW143296	*Mad2l1*	1398602_at	203362_s_at	*MAD2L1*
NM_019318	*Maf*	1385243_at	209348_s_at	*MAF*
NM_019318	*Maf*	1385243_at	209347_s_at	*MAF*
NM_019318	*Maf*	1385243_at	206363_at	*MAF*
AI714002	*Mki67*	1374775_at	212022_s_at	*MKI67*
AI714002	*Mki67*	1374775_at	212023_s_at	*MKI67*
AI714002	*Mki67*	1374775_at	212021_s_at	*MKI67*
AI714002	*Mki67*	1374775_at	212020_s_at	*MKI67*

Table W1. (*continued*)

Rat Accession Number	Rat Gene Symbol	Rat 230 2.0 Probe Set	Human HG-U133A Probe Set	Human Gene Symbol
BE115673		1392086_at	203037_s_at	*MTSS1*
BE115673		1392086_at	203036_s_at	*MTSS1*
BE115673		1392086_at	210360_s_at	*MTSS1*
BE115673		1392086_at	210359_at	*MTSS1*
NM_012603	*Myc*	1368308_at	202431_s_at	*MYC*
BI300996	*Mycl1*	1395781_at	214058_at	*MYCL1*
BI300996	*Mycl1*	1395781_at	215491_at	*MYCL1*
NM_133583	*Ndrg2*	1387121_a_at	214279_s_at	*NDRG2*
NM_133583	*Ndrg2*	1387121_a_at	214278_s_at	*NDRG2*
NM_133583	*Ndrg2*	1387121_a_at	206453_s_at	*NDRG2*
BG666709	*Ndr4*	1370229_at	209159_s_at	*NDRG4*
NM_021589	*Ntrk1*	1369000_at	208605_s_at	*NTRK1*
NM_019210	*Pak3*	1368902_at	214607_at	*PAK3*
U05989	*Pawr*	1368702_at	204005_s_at	*PAWR*
U05989	*Pawr*	1368702_at	204004_at	*PAWR*
U05989	*Pawr*	1368702_at	214237_x_at	*PAWR*
U05989	*Pawr*	1368702_at	214090_at	*PAWR*
BE100812	*Pdgfa*	1379375_at	205463_s_at	*PDGFA*
BE100812	*Pdgfa*	1379375_at	216867_s_at	*PDGFA*
NM_031317	*Pdgfc*	1392274_at	218718_at	*PDGFC*
BM389426	*Pdgfrb*	1370642_s_at	202273_at	*PDGFRB*
BM384311		1374616_at	205226_at	*PDGFRL*
U10188	*Plk1*	1370297_at	202240_at	*PLK1*
U10188	*Plk1*	1370297_at	201429_s_at	*PLK1* (*RPL37A*)
BE109322	*Plk4*	1377832_at	204886_at	*PLK4*
BE109322	*Plk4*	1377832_at	204887_s_at	*PLK4*
BE109322	*Plk4*	1377832_at	211088_s_at	*PLK4*
NM_013196	*Ppara*	1394800_at	210771_at	*PPARA*
NM_013196	*Ppara*	1394800_at	206870_at	*PPARA*
NM_013124	*Pparg*	1369179_a_at	208510_s_at	*PPARG*
AA891940	*Arhc*	1371659_at	200885_at	*PPM1J*
BI282953	*Pycard*	1389873_at	221666_s_at	*PYCARD*
NM_053459	*Rab27b*	1370122_at	207017_at	*RAB27B*
NM_053459	*Rab27b*	1370122_at	207018_s_at	*RAB27B*
AA924620	*Rab40b*	1383826_at	204547_at	*RAB40B*
AA924620	*Rab40b*	1383826_at	217597_x_at	*RAB40B*
AI409259	*Racgap1*	1373658_at	222077_s_at	*RACGAP1*
BF284067		1373631_at	203911_at	*RAP1GAP*
BF284067		1373631_at	210618_at	*RAP1GAP*
NM_133410	*Rap2b*	1392922_at	213923_at	*RAP2B*
NM_133410	*Rap2b*	1392922_at	214487_s_at	*RAP2B*
NM_133410	*Rap2b*	1392922_at	214488_at	*RAP2B*
AI237779	*Rasa3*	1392224_at	206221_at	*RASA3*
AI237779	*Rasa3*	1392224_at	206220_s_at	*RASA3*
AW532114	*Rasgrp2*	1374872_at	214367_at	*RASGRP2*
AW532114	*Rasgrp2*	1374872_at	214368_at	*RASGRP2*
AW532114	*Rasgrp2*	1374872_at	214369_s_at	*RASGRP2*
AW532114	*Rasgrp2*	1374872_at	208206_s_at	*RASGRP2*
AA955648	*Arhd*	1382197_at	209885_at	*RHOD*
AA955648	*Arhd*	1382197_at	31846_at	*RHOD*
BE097238	*RICS*	1377061_at	210791_s_at	*RICS*
BE097238	*RICS*	1377061_at	203431_s_at	*RICS*
AI706777	*Rin3*	1375020_at	60471_at	*RIN3*
AI706777	*Rin3*	1375020_at	219457_s_at	*RIN3*
AI706777	*Rin3*	1375020_at	219456_s_at	*RIN3*
AI706777	*Rin3*	1375020_at	220439_at	*RIN3*
AI144754	*Rnd1*	1381533_at	210056_at	*RND1*
AI235414		1377029_at	210479_s_at	*RORA*
AI235414		1377029_at	210426_x_at	*RORA*
BE110171		1379833_at	206419_at	*RORC*
NM_021865	*Jundp1*	1369891_at	220358_at	*SNFT*
NM_021578	*Tgfb1*	1370082_at	203085_s_at	*TGFB1*
NM_021578	*Tgfb1*	1370082_at	203084_at	*TGFB1*
NM_031131	*Tgfb2*	1387172_a_at	220407_s_at	*TGFB2*
NM_031131	*Tgfb2*	1387172_a_at	209908_s_at	*TGFB2*
NM_031131	*Tgfb2*	1387172_a_at	220406_at	*TGFB2*
BI283829	*Hdgfrp3*	1379482_at	219892_at	*TM6SF1*
NM_012870	*Tnfrsf11b*	1369407_at	204933_s_at	*TNFRSF11B*
NM_012870	*Tnfrsf11b*	1369407_at	204932_at	*TNFRSF11B*
BI303379	*Tnfrsf12a*	1371785_at	218368_s_at	*TNFRSF12A*
AA800814	*Tnfsf13*	1377353_a_at	210314_x_at	*TNFSF13*
AA800814	*Tnfsf13*	1377353_a_at	209500_x_at	*TNFSF13*

Table W1. (*continued*)

Rat Accession Number	Rat Gene Symbol	Rat 230 2.0 Probe Set	Human HG-U133A Probe Set	Human Gene Symbol
AA800814	*Tnfsf13*	1377353_a_at	209499_x_at	*TNFSF13*
AA800814	*Tnfsf13*	1377353_a_at	211495_x_at	*TNFSF13*
AA900477		1384170_at	205537_s_at	*VAV2*
AA900477		1384170_at	205536_at	*VAV2*
NM_053653	*Vegfc*	1368463_at	209946_at	*VEGFC*
NM_031534	*Wt1*	1369695_at	206067_s_at	*WT1*
NM_031534	*Wt1*	1369695_at	216953_s_at	*WT1*

Mouse Accession Number	Mouse Gene	Mouse MG-74Av2 Probe Set	Rat Accession Number	Rat Gene Symbol	Rat 230 2.0 Probe Set	Human HG-U133A Probe Set	Human Gene Symbol
AF002823	*Bub1*	104097_at	BF388785	*Bub1*	1385086_at	209642_at	*BUB1*
AF002823	*Bub1*	104097_at	BF388785	*Bub1*	1385086_at	216277_at	*BUB1*
AF002823	*Bub1*	104097_at	BF388785	*Bub1*	1385086_at	216275_at	*BUB1*
AF002823	*Bub1*	104097_at	BF388785	*Bub1*	1385086_at	215509_s_at	*BUB1*
AF002823	*Bub1*	104097_at	BF388785	*Bub1*	1385086_at	215508_at	*BUB1*
X75483	*Ccna2*	99186_at	AA998516	*Ccna2*	1379582_a_at	213226_at	*CCNA2*
X75483	*Ccna2*	99186_at	AA998516	*Ccna2*	1379582_a_at	203418_at	*CCNA2*
X66032	*Ccnb2*	94294_at	AW253821	*Ccnb2*	1389566_at	202705_at	*CCNB2*
AI849928	*Ccnd1*	94232_at	X75207	*Ccnd1*	1371150_at	208712_at	*CCND1*
AI849928	*Ccnd1*	94232_at	X75207	*Ccnd1*	1371150_at	208711_s_at	*CCND1*
M38724	*CDC2a*	100128_at	NM_019296	*Cdc2a*	1367776_at	203213_at	*CDC2*
M38724	*CDC2a*	100128_at	NM_019296	*Cdc2a*	1367776_at	210559_s_at	*CDC2*
M38724	*CDC2a*	100128_at	NM_019296	*Cdc2a*	1367776_at	203214_x_at	*CDC2*
AW061324	*CDC20*	96319_at	U05341	*Cdc20*	1387895_s_at	202870_s_at	*CDC20*
AV138783	*Gadd45b*	161666_f_at	BI287978	*Gadd45b*	1372016_at	207574_s_at	*GADD45B*
AV138783	*Gadd45b*	161666_f_at	BI287978	*Gadd45b*	1372016_at	209305_s_at	*GADD45B*
AV138783	*Gadd45b*	161666_f_at	BI287978	*Gadd45b*	1372016_at	209304_x_at	*GADD45B*
AV138783	*Gadd45b*	161666_f_at	BI287978	*Gadd45b*	1372016_at	213560_at	*GADD45B*
U83902	*Mad2l1*	99632_at	AW143296	*Mad2l1*	1398602_at	203362_s_at	*MAD2L1*
AB033921	*Ndr2*	96088_at	NM_133583	*Ndrg2*	1387121_a_at	214279_s_at	*NDRG2*
AB033921	*Ndr2*	96088_at	NM_133583	*Ndrg2*	1387121_a_at	214278_s_at	*NDRG2*
AB033921	*Ndr2*	96088_at	NM_133583	*Ndrg2*	1387121_a_at	206453_s_at	*NDRG2*
U01063	*Plk*	93099_f_at	U10188	*Plk1*	1370297_at	202240_at	*PLK1*
U01063	*Plk*	93099_f_at	U10188	*Plk1*	1370297_at	201429_s_at	*PLK1* (*RPL37A*)
AW122347	*Racgap1*	94953_at	AI409259	*Racgap1*	1373658_at	222077_s_at	*RACGAP1*